

Nitrogen Doping and Infusion in SRF Cavities: A Review

Pashupati Dhakal*

Thomas Jefferson National Accelerator Facility, Newport News, VA 23606, USA

Abstract

Advances in SRF technology over the last 40 years allowed achieving accelerating gradients ~ 50 MV/m corresponding to peak surface magnetic field close to the theoretical limit of niobium. However, the quality factor was found to decrease significantly with increasing accelerating gradient. This is somewhat expected since increasing the rf field increases the number of quasiparticles and therefore the rf losses. Recently, a phenomenon has been observed in which there is an increase in quality factor with the accelerating gradient when the cavities are doped with certain non-magnetic impurities. In particular, the diffusion of nitrogen into the niobium cavities inner surface has been successfully implemented into the commercialization of SRF technology. The quest is still ongoing towards process development to achieve high accelerating gradient SRF structures with high quality factors for future high power accelerators. Here, we present the review of the research and development via nitrogen diffusion, materials analysis and current theoretical understanding in high Q_0 SRF cavities.

I. Introduction

Superconducting radiofrequency (SRF) technology is being used not only for the basic fundamental nuclear physics research but also for applications that have benefited society [1]. Most of the future accelerating machines in large or compact systems completely rely on the SRF technology. Few examples of the current and future projects based on accelerator technology are continuous wave (CW) free electron lasers, x-ray laser oscillators, ERL based light sources, short photon pulses in storage ring light sources, electrons and ions colliders, accelerator driven system (ADS) for medical isotope production and nuclear waste transmutation. SRF technology which is based on the superconducting hollow structures (cavities) with high duty factor provides the required accelerating gradient to accelerate the charge particles close to the velocity of light.

* Email: dhakal@jlab.org

The superiority of superconducting cavities over the normal metal cavities is its ability to store the large amount of energy with much lower dissipation. The performance of the SRF cavities are measured in terms of the quality factor $Q_0 = G/R_s$, where G is the geometric factor which depends on the cavity geometry and R_s is the surface resistance, as a function of accelerating gradient, E_{acc} . For typical cavities of resonating frequency 0.5–3 GHz operating at a temperature ~ 2.0 K the quality factor is in the 10^{10} – 10^{11} range. In the last four decades, much research work has been done to improve the accelerating gradient and quality factor of these SRF cavities. The theoretical gradient limit on these cavities which is limited by the superheating field has been achieved in some occasions and great effort has been put on pushing the quality factor to higher values. Historical landscape of the R&D of L-band SRF cavity on single and multi-cell cavities is shown in Fig. 2. Higher Q_0 for the reduction of losses (lower cooling capacity) and higher E_{acc} for high energy and compact accelerators are desired (Fig. 1). Currently under constructions and proposed accelerators such as FRIB, ILC, XFEL, LCLS-II, ADS and ERLs have different specifications for the gradient and quality factor. Machines such as ILC and XFEL are designed to be operated in pulse mode whereas LCLS-II, ADS and ERLs are designed to operate in CW mode [2,3]. For the CW applications, the reliable and affordable cryogenic refrigeration system currently limits the optimal gradient to ~ 20 MV/m for long term accelerator operation. The continuous research and development already pushed the achievable accelerating gradient towards the fundamental limits [4].

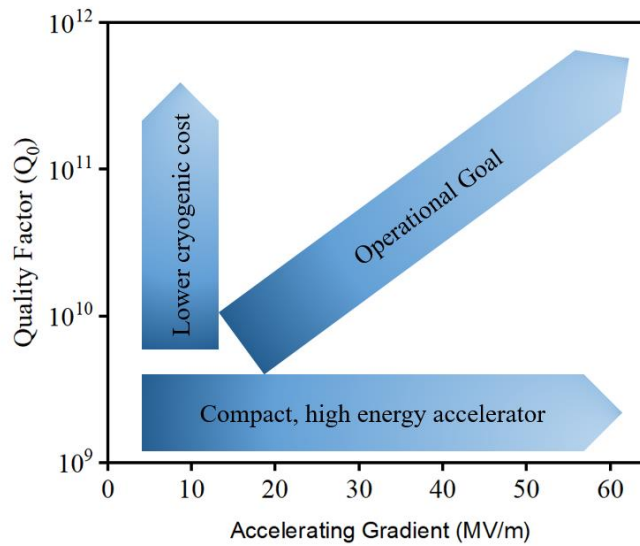


Figure 1. Schematic of SRF cavity performances.

Thus current and future accelerators would highly benefit from cavities with higher quality factor and gradient. Higher quality factor can be achieved by minimizing the surface resistance of SRF cavities. Surface resistance in superconducting materials is the sum of the temperature independent residual resistance (R_{res}) and temperature dependent Bardeen-Cooper-Schrieffer (BCS) resistance (R_{BCS}) [5,6]. The sources of the R_{res} are trapped magnetic flux during the cavity cool down, impurities, hydrides and oxides, imperfections, and surface contamination. The BCS surface resistance results from the interaction between the RF electric field within the penetration depth and thermally activated quasi-particles in the superconductor. The BCS surface resistance depends on superconducting material parameters which may vary strongly due the presence of the metallic impurities within the rf penetration depth.

In the past almost a decade, much progress has been made in the development of the high quality factor SRF cavities via the material diffusion in the thin layer of inner surface of the cavities. The possibilities of higher quality factor in SRF cavities were first realized by the titanium doping during annealing (~ 1400 °C) without any post-annealing chemistry [7,8] and later by nitrogen doping at 800 °C, followed by electropolishing [9]. The diffusion process not only showed the increase in quality factor at low field levels, but also an increase in quality factor with increasing accelerating gradient, contrary to the previously observed Q -slope. The nitrogen doping recipe rapidly implemented into the industrialization of the technology in processing of SRF cavities for LCLS-II cryomodules production. One of the challenge faced during the cavity processing is the degradation of the accelerating gradient after the nitrogen doping compared to the gradient limit would have been achieved with the available processing technique available to that date.

Most recently, efforts have been made to preserve high accelerating gradients while also increasing the quality factor of SRF cavities. In these new nitrogen “infusion” cavity processing recipes, cavities were heat treated at high temperature (>800 °C), then the furnace temperature is reduced to 120–200 °C and nitrogen is introduced into the furnace at a partial pressure of ~ 25 mTorr for several hours. This process has shown an improvement in Q_0 over the baseline measurements, without the need for postannealing chemical removal of material from the inner surface [10,11,12]. Even though diffusion of the nitrogen into the bulk of the SRF cavity is limited in depth at these low temperature, the introduction of nitrogen is sufficient to modify the cavity surface within the rf penetration depth as seen from rf results, which are similar to those previously

performances. In section VII, we present the available theoretical models that explains the high Q and high gradient cavity performances. Section VIII presents the summary and future outlooks.

II. Nitrogen Doping

Over the last several decades, several attempt were made to increase the quality factor of SRF cavities. Initially with the issue with the hydrogen being the show stopper, still to some extent, attempt were made to surface passivation with the growth of oxides [15] and nitrides [16,17]. The idea behind these surface passivation is to avoid the reabsorption of hydrogen on the bulk of niobium such that the surface is transparent to rf field without dissipating any extra rf power. The surface oxidation experiments were carried out at high temperature showed the enhanced Q [15], Furthermore, an additional titanium impurities during the high temperature heat treatment change the paradigm of SRF cavities performance with increase in quality factor with the accelerating gradient [7,8].

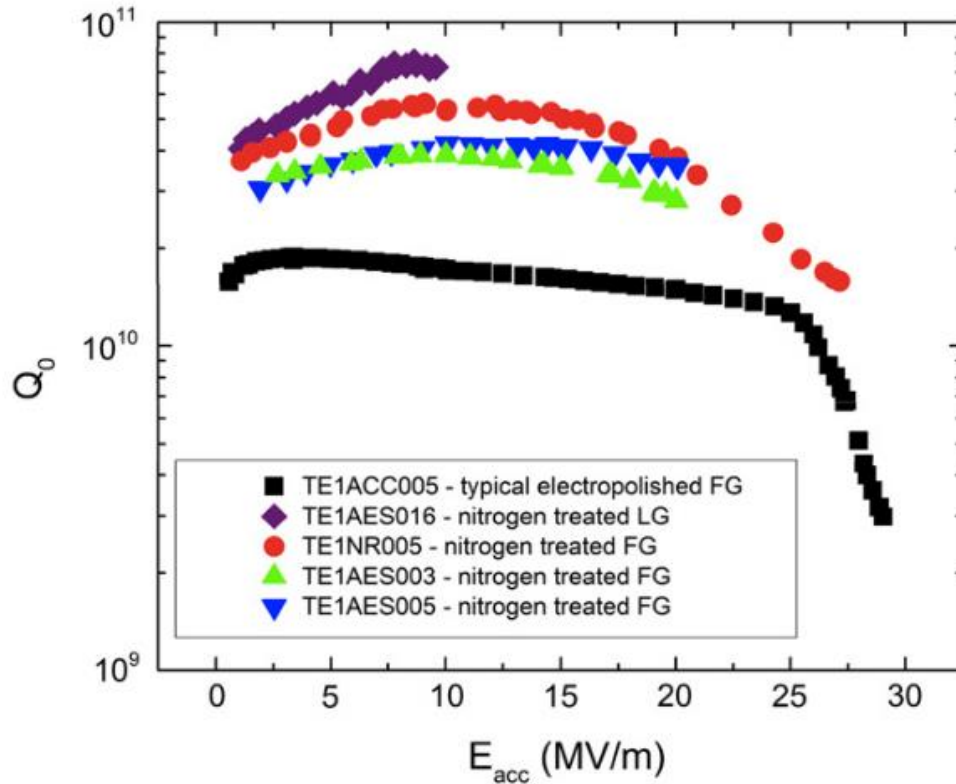


Figure 3. First demonstration of increase in quality factor after nitrogen doping followed by electropolishing on cavity made from fine grain and large grain niobium [9].

The similar experimental exploration was carried out at Fermi Lab in 2013 in an attempt to form niobium nitride on the inner surface of SRF cavity by reacting bulk niobium cavities with nitrogen in a high temperature UHV furnace as shown in Fig. 3 [9]. Even though, the effort to achieved higher quality factor due to formation niobium nitride was not successful, the discovery was made with the increase in quality factor with accelerating gradient when inner surface of the cavity was removed by electropolishing. The $Q_0(E_{acc})$ curve showed the anti-Q-slope similar to that was observed when the cavity was heat treated at high temperature in titanium environment [7,8]. It was concluded that the interstitial diffusion of the non-magnetic impurities (Ti and N) indeed enhance the quality factor by decrease in BCS surface resistance as the accelerating gradient increases.

III. Recipe Development

After the demonstration of exceptionally high quality factor on nitrogen doped SRF single cell cavities, the focus quickly shifted to the application of nitrogen doped cavities in superconducting linear accelerator. Around the same time, the Linac Coherent Light Source-II (LCLS-II) project quickly adopted the nitrogen doped SRF cavities to be installed in cryomodules [18]. The LCLS-II baseline design required 1.3 GHz 9-cell TESLA shaped cavities [19] with an average intrinsic quality factor $Q_0 \sim 2.7 \times 10^{10}$ with accelerating gradient of 16 MV/m at 2.0 K [20]. Joint LCLS-II R&D efforts among different laboratories towards achieving the high quality factor were started with aiming towards the development of the cavity processing technique that can be commercially produced in large numbers [21]. Three partner labs to LCLS-II projects: Fermi Lab, Jefferson Lab and Cornell University rapidly developed separate recipe with nitrogen doping on single cell cavities and were successfully applied to 9-cell cavities [22,23,24,25].

A. Furnace Requirement

Generally most of the SRF facilities are equipped with the furnace capable of going as high as 1250 °C with resistive heaters. The SRF facilities at Fermi Lab [26], Jefferson Lab [27] and Cornell University [28] used furnace manufactured by TM vacuum [29]. These furnace are equipped with dry roughing pump, cryopumps, residual gas analyzers, vacuum gauges and gas injection system. The high purity nitrogen (> 99.9999%) is used during the doping process with the flow controlled by mass flow controller. Typically, the temperature of the furnace is ramped up to desired

temperature (800-1000 °C) at the rate of 3-5 °C/min and hold for few hours (~3 hours), mainly for the hydrogen degassing purpose. At the end of degassing cycle, high purity nitrogen gas is injected for a period of time (2-30 min), also called soaking time, with specified partial pressure of nitrogen. During the early stage of doing recipe development, the gas was turned off, the furnace was evacuated and the furnace was naturally cooldown to the room temperature. Later the recipe is modified in such a way that after the soaking time, the furnace was evacuated and let the cavity further anneal before cooling down to room temperature. For example, a research group at KEK initially weren't able to reproduce the doping results [30] and with the improvement on the furnace pumping system, they successfully reproduced the doping results [31].

B. Nitrogen Diffusion

Thermal diffusion of nitrogen into Nb is a method which had been used in the past to produce NbN films [32,33,34], with higher superconducting transition temperature than Nb. Earlier attempts to produce the nitride phase for surface passivation in SRF cavities didn't result in the Q-rise phenomenon, however the overall increase in quality factor was observed in all accelerating gradient when the SRF cavities were heat treated in nitrogen environment at temperature ~400 °C with partial pressure of $\sim 10^{-5}$ mTorr [17]. The study suggested that the temperature and partial pressure of nitrogen was insufficient to diffuse in to the bulk of niobium or formation of any nitride phase in the surface of niobium.

Historically, Nb-N system is interesting because of the superconducting behavior of the δ -NbN_{1-x} phase and of its extension into ternary phases such as (Ti, Nb)N_{1-x} [35]. Several complex phase of Nb-N are observed depending on the ratio of niobium and nitrogen (stoichiometric) as shown in Fig. 4 and nitrogen can diffuse on the interstitials of niobium deeper in to the surface [36]. From the phase diagram, the phase of the nitride on niobium is determined by the concentration of the nitrogen and temperature of niobium substrate [37,38]. The apparent activation energy during the nitrogen diffusion decreases with increasing temperature up to about 650 °C. Then it stays constant up to 1300 °C, above which it increases to a new value of 50 kcal/mol [39]. Most of the diffusion data available in literature are done at higher temperature with most on atmospheric nitrogen pressure on sample coupons as shown in Fig. 5.

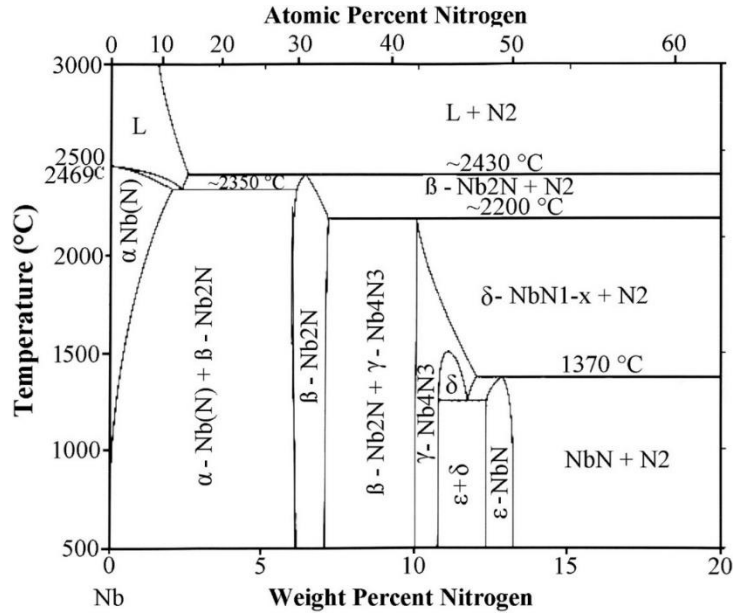


Figure 4. Nb-N Phase diagram, taken from Ref. [36]

The nitrogen doping parameters during the first demonstration on SRF cavities was random. However, the questions raised about the diffusion mechanism of nitrogen on the niobium. The diffusion of the nitrogen in niobium usually starts with the formation of stoichiometric nitride phase on the surface and diffusion of the nitrogen in the bulk takes place. Depending on the temperature and amount of nitrogen being introduced on the surface of niobium, the diffusion of nitrogen can be few to hundred micrometers [40, 41, 42, 43]. The nitride features are clearly visible on the surface of niobium and those are identified as Nb₂N with TEM analysis [44] as well as XPS measurements [45, 46] consistent with the earlier observations of sub nitride having a composition of hexagonal Nb₂N [47]. Tetragonal, a face-centered cubic, and two hexagonal nitrides having compositions of NbN_{0.75} to NbN were also observed in earlier studies when nitrogen diffusion was done at atmospheric pressure and at higher temperature [48]. At the temperature of interest for SRF cavities, very small amount of nitrogen will diffuse to the bulk of the Nb and most forms nitride layers on the surface starting at temperature as low as 400 °C [49].

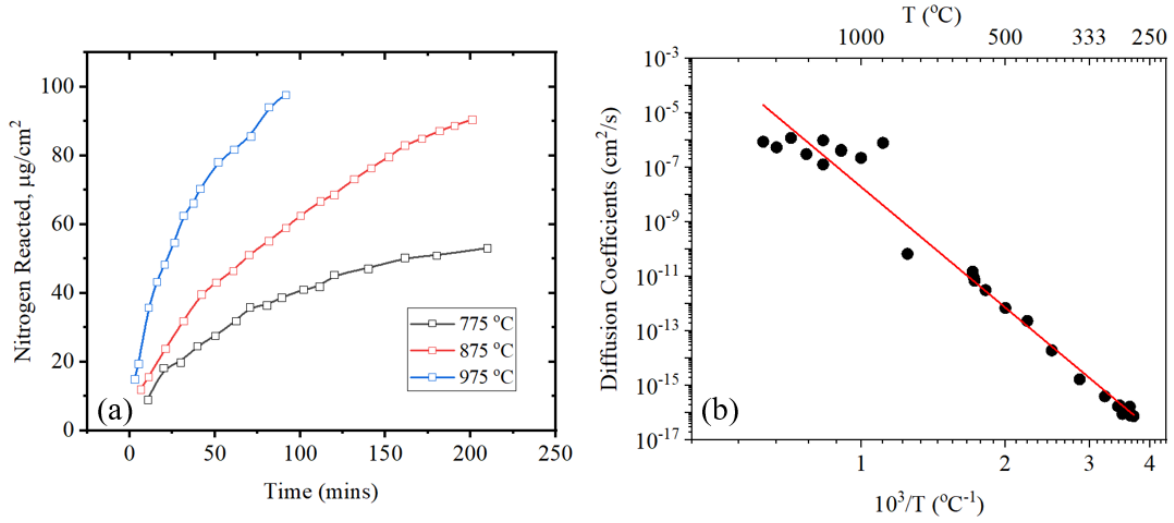


Figure 5. (a) Reaction rate of nitrogen in atmospheric pressure [48]. (b) Nitrogen diffusion as a function from temperature [38].

There is very limited work been done on the crystal orientation dependence on the diffusion on nitrogen on SRF niobium [40, 50]. Since niobium is a body centered cubic structure, which should not exhibit diffusion profile based on the crystal orientation. The doping study done cavities made from large grain niobium also showed the improve Q as good as cavity made from fine grain niobium, if not better [9, 43, 51,52]. No performance enhancement was observed on cavity made from low purity niobium, probably due to the higher concentration of impurities preventing the optimal diffusion of nitrogen in the bulk [43]. However, more systematic studies are still needed on the diffusion of nitrogen in niobium with respect to the temperature, partial pressure of nitrogen, duration of diffusion and the metallurgical state of niobium.

C. Electropolishing

One of the required steps after the nitrogen doping in order to achieve high quality factor is controlled electropolishing on inner surface of cavity. However, a recent study on single cell cavity also showed an encouraging result when the post doping material removal by buffer chemical polishing (BCP) [53]. Historically, the EP process is applied to achieve a smoother cavity surface and found to be superior to the BCP process and accelerating gradient can be enhanced with low temperature baking in UHV environment [54]. The standard EP acid mixture contains nine volume parts of sulphuric acid H_2SO_4 (96%) and 1 part of hydrofluoric acid HF (48%). EP is

a surface finishing process whereby the anodization of Nb by H_2SO_4 forces the growth of Nb_2O_5 and F^- dissolves Nb_2O_5 . A lot of progress was made in optimizing the electropolishing technique over the years [55, 56, 57, 58]. The typical horizontal electropolishing systems consists of the cathode-anode set up with cavity being anode and aluminum cathode inserted along the cavity axis as shown in Fig. 6. The I-V characteristics, temperature of the EP mixtures, temperature of cavity surface plays the significant role in etching or polishing the niobium surface. The details on process development can be found in Ref. 59.

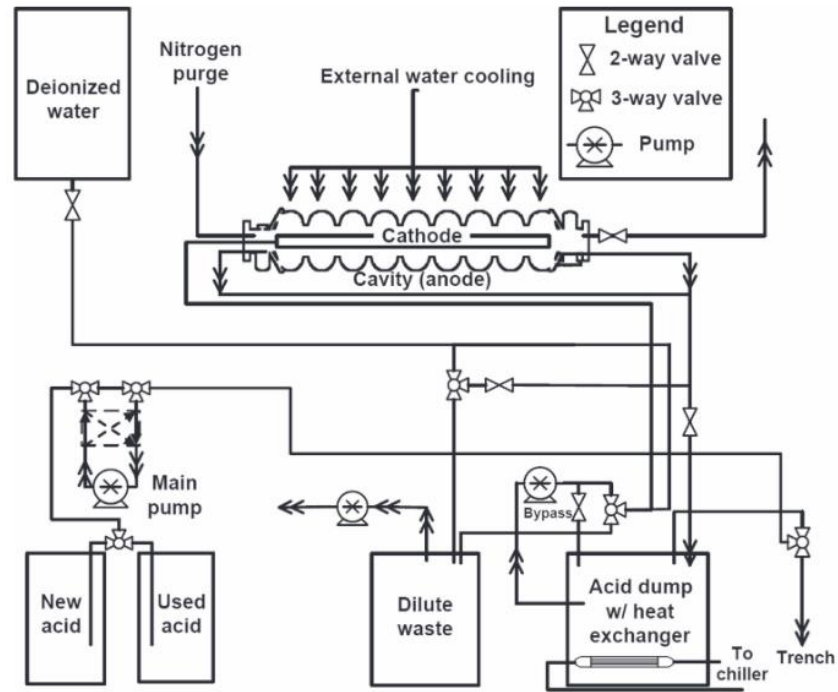


Figure 6. Schematic flow chart for a cavity electropolishing system [54].

The effect of amount of material removal on the performance of nitrogen doped cavities were studied in details [21-28]. It is found that the accelerating gradient increases while decreasing the overall quality factors as more material was removed from the cavity's inner surface, especially in heavy doped SRF cavities (20N30 recipe) as shown in Fig. 7. This confirms the fact that some optimal nitrogen concentration is needed for high Q_0 , however the gradient is limited to the lower values. However, no definitive answer to the relationship of material removal, Q_0 and E_{acc} is available, it is believed that the early cavity quench due to the large segregation of nitrogen on localized size, driving the region into normal conducting state. Further removal of material may

reduce the localized site but the overall concentration of nitrogen is lower and superconducting properties approach the clean limit.

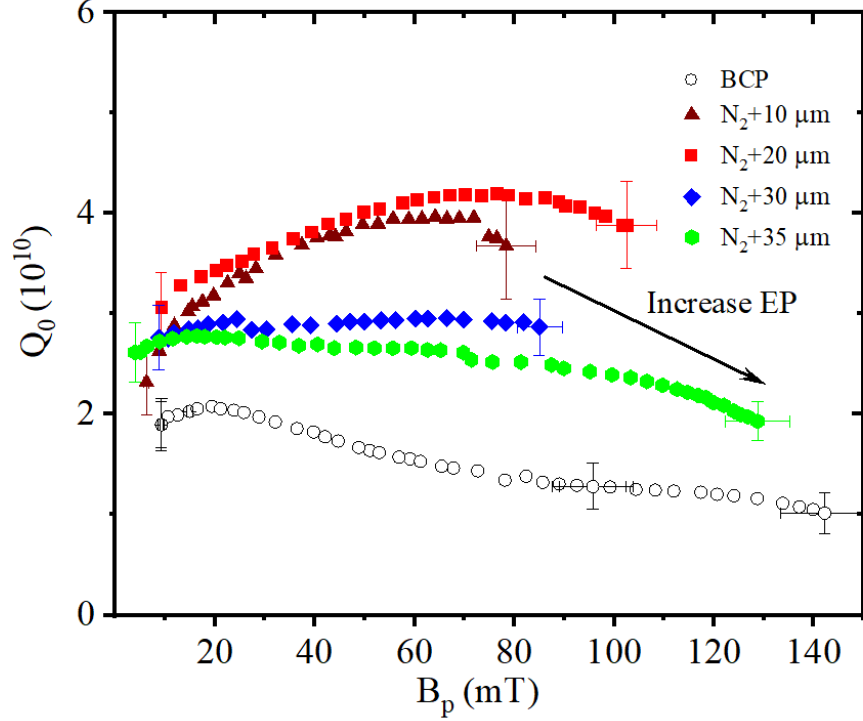


Figure 7. The effect of successive EP on single cell cavity ($B_p/E_{acc} = 4.23 \text{ mT}/(\text{MV}/\text{m})$) with nitrogen doped with 20N30 recipe [51]. The accelerating gradient increase with increasing the EP removal, while decreasing the overall quality factor.

IV. Industrialization

The initial research and development on nitrogen doping was limited in Fermi Lab, Jefferson Lab and Cornell University. The research group working closely started the work in single cell cavity on recipe development changing the nitrogen diffusion time[†]. Some details of the recipe development is already mentioned in section III, A. Several trials were done on the exposure and annealing time in order to identify the best recipe that met the LCLS-II cavity performance specifications. A recipe 2N6 (2 minutes nitrogen exposure followed by 6 minutes of annealing in UHV environment) was chosen to be used in the project and technology was

[†] In literature, the recipe is usually defined as xNy, where x (1-30 mins) represents the nitrogen diffusion time and y (0-60 mins) represent the annealing time in minutes in UHV environment.

transferred to the cavity manufacturers Research Instruments and Zanon. The electropolishing technology was transferred from Jefferson lab to the vendor sites.

The niobium for cavity fabrications was obtained from Tokyo Denkai and Ningxia with similar material specification as XFEL [60]. Total 373 cavities were ordered and tested at Jefferson Lab and at Fermi Lab showed an excellent performance with average accelerating gradient 22.0 ± 3.6 MV/m with quality factor $(3.1 \pm 0.5) \times 10^{10}$ as shown in Fig. 8 [61,62]. The successful production of several hundred cavities with nitrogen doping proved the reproducibility of the technological development within short period of time. Even though, the nitrogen doping was successfully applied to several multi cell cavities in mass production, several recipe modifications were made during the production [62]. Among them are; issue with electropolishing and annealing process of cavities prior to the nitrogen doping. The electropolishing issue were mitigated by the improved cathode and parameters with the help of Jefferson lab researchers [61].

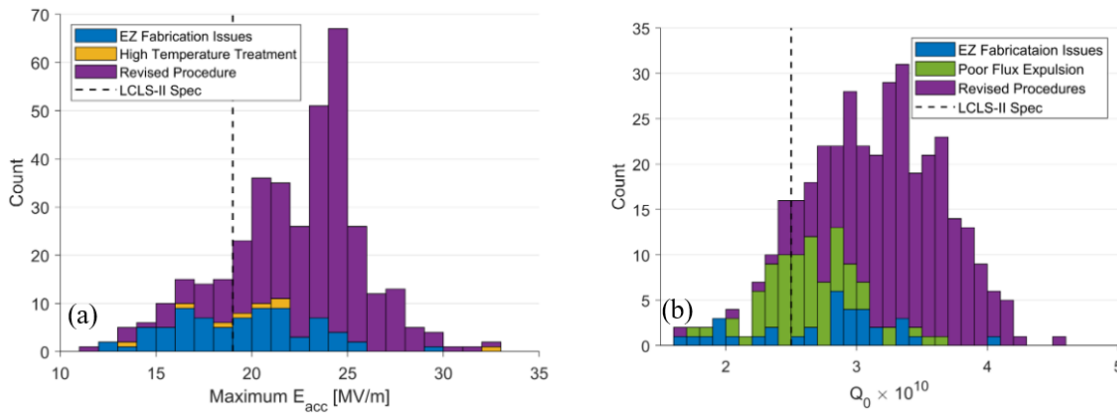


Figure 8. Summary of performance of LCLS-II cavities (~373 cavities) in vertical test on cavities commercially produced in two different vendor sites, from raw Nb materials from two different vendors. The cavities were doped with 2N6 recipe followed by 5-7 μm EP at vendor sites [61].

In order to achieve the high quality factor in SRF cavities, one has to minimize the trapped residual magnetic field during the cooldown of SRF cavities. It was found that high temperature gradient along the cavity is needed during the cooldown when the cavity surface temperature transition from normal conducting to the superconducting state (~ 9.2 K). This is needed in order to expel magnetic field from the SRF cavities due to Meissner effect, leading to the lower residual resistance due to trapped magnetic field [63,64,65,66]. Furthermore, these doped cavities are more vulnerable to flux pinning, extra care is needed to minimize any intrinsic source of pinning center. During the production of LCLS-II cavities, several cavities' quality factor was limited by the poor

flux expulsion. Even though, the material specification from different vendors were the same, the performance of the cavities made from the two vendors showed different flux expulsion. In the middle of the production, additional R&D was done in order to optimize the maximum flux expulsion with increasing annealing temperature prior to the doping process. The cavities annealed at higher temperature (900-975 °C) showed much better flux expulsion compared to 800 °C annealed cavities [62, 67]. Study also showed that the grain size may also plays the significant role in flux expulsion [67].

The rapid progress on development of SRF cavities with nitrogen doping was mainly due to the requirement for LCLS-II project. As a parts of R&D and possible use in future accelerator projects, nitrogen doping work were carried out in other part of the world, mainly in KEK Japan [31, 68], IHEP [69] and PKU in China [70,71]. Currently, the nitrogen doping technology is considered to be used in Shanghai Coherent Light Facility (SHINE) similar to LCLS-II project.

V. Towards High Q_0 and High Gradient

The nitrogen doping provided the a avenue for the future accelerators operations due to the high quality factors, specifically, the CW accelerators which are operated with accelerating gradient of ≤ 20 MV/m. Coincidentally, most of the SRF cavities are limited at lower accelerating gradient ≤ 20 MV/m much lower than what would have been achieved without doping. For example, the average accelerating gradient of 743 cavities used in XFEL projects was 31.4 ± 6.8 MV/m [72,73] with conventional (pre doping era) cavity processing recipe. During the LCLS-II cavity production, the average accelerating gradient of ~ 375 cavities was 22.0 ± 3.6 MV/m [Dan TTC 2020]. This shows $\sim 30\%$ reduction on achievable maximum accelerating gradient. However, the benefits of higher Q_0 at accelerating gradient $E_{acc} \sim 20$ MV/m, clearly shows the benefits of using doped cavities in CW machine.

Future accelerators such as International Linear Collider (ILC) will require high gradient and the project will benefit with high Q_0 SRF cavities [74]. Moreover the proposed upgrade of LCLS-II program is also increasing its operation specification to higher gradient show the further R&D in order to increase the accelerating gradient with high Q_0 SRF cavities.

A. High Temperature Doping

One of the route to increase the accelerating gradient currently being pursued is to use of the modified nitrogen doping recipe with varying the nitrogen diffusion and annealing time. Once again with the LCLS-II HE project driven R&D conducted independently at Jefferson Lab and Fermi Lab are currently pursuing a different doping recipe. Jefferson Lab explored the low doping recipe where the nitrogen was introduced in the furnace for short period of time (2-3 minutes) followed by longer annealing time (~60 mins). The hypothesis behind this recipe is that the nitrogen will diffuse deeper in the bulk with uniform concentration, leading to high accelerating gradient. Recipe applied to single cell cavities reached ~35 MV/m, however with the high field Q-slope [75]. Further optimization on doping infrastructure with capping cavities opening with Nb foils, smoother pre-doping surface and colder electropolishing led to initial results on 9-cell cavities accelerating gradient closer to 30 MV/m [62,67].

Fermi Lab explored the recipe different than that was being considered by Jefferson Lab in order to increase the accelerating gradient on doped cavities. The proposed recipe include the short nitrogen diffusion time (~2 mins) with no post annealing time. The preliminary results on single cell showed the accelerating gradient above 25 MV/m with high field Q-slope, similar to that has been observed with Jefferson Lab 3N60 recipe as shown in Fig. 9. With available 9-cell cavity test results, using 2N0 recipe, there is small increase in accelerating gradient (~ 3 MV/m) over the earlier 2N6 recipe [76]. Further R&D are being planned to increase the accelerating with high Q_0 in doped cavities in order to realization of LCLS high energy upgrade [77].

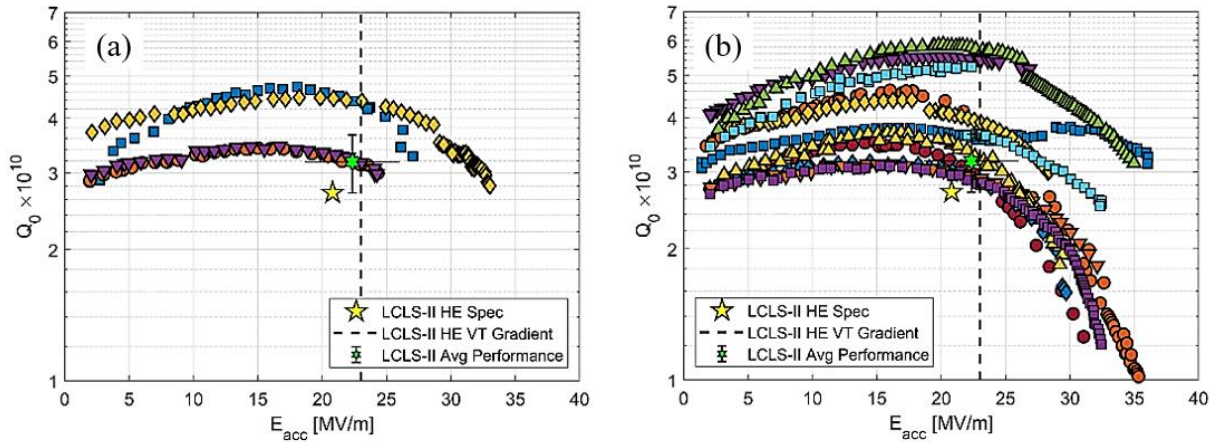


Figure 9. $Q_0(E_{acc})$ of single cell cavities with modified recipe (a) 2N0 and (b) 3N60, in order to achieve high Q_0 , high gradient SRF cavities aim for LCLS-II-HE project [61].

B. Recipe Development at Low Temperature

Alternative to the nitrogen doping at high temperature followed by the electropolishing to control the optimal nitrogen concentration within the rf penetration depth was realized using nitrogen with the recipe involved at low temperature baking [10]. In these new nitrogen “infusion” cavity processing recipes, cavities were heat treated at 800 °C for ~3 hours and the furnace temperature is reduced to 120-300 °C. The nitrogen is introduced into the furnace at a partial pressure of ~ 25 mTorr for several hours (24-96 hours) in the temperature range of 120-200 °C. This process has shown an improvement in Q_0 over the baseline measurements, without the need for post-furnace electropolishing [11,12,78, 79,80,81,82]. The summary of single cell cavity results is shown in Fig. 10.

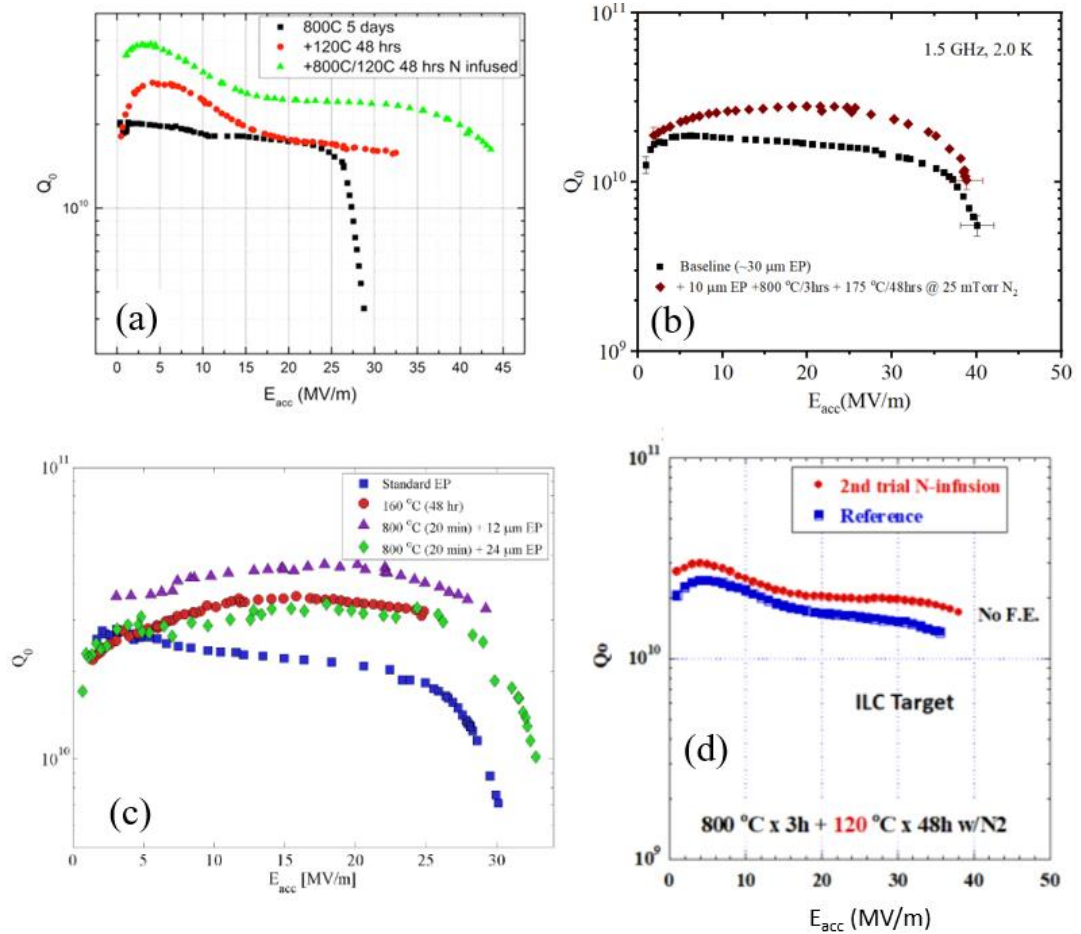


Figure 10. The quality factor of single cell SRF cavities with nitrogen infusion, at (a) Fermi Lab [10], (b) Jefferson Lab [12], (c) Cornell University [11] and (d) KEK [80].

In particular at Jefferson lab, the benefits in nitrogen doping was observed when the nitrogen gas is injected into the furnace at elevated temperature ($\sim 250\text{-}300\text{ }^{\circ}\text{C}$) and let the cavity cooldown to lower temperature ($120\text{-}200\text{ }^{\circ}\text{C}$) and hold at that temperature for extended period of times (24 - 48 hours) [12, 83]. Even though diffusion of the nitrogen into the bulk of the SRF cavity is limited in depth at these low temperatures ($120\text{-}200\text{ }^{\circ}\text{C}$), the introduction of nitrogen is sufficient to modify the cavity surface within the rf penetration depth as seen from cavities' test results, which are similar to those previously reported for high-temperature nitrogen doped cavities. The nitridation and diffusion of nitrogen into the bulk is expected when the Nb surface is free of Nb_2O_5 which occurs $>300\text{ }^{\circ}\text{C}$ [84,85], but the infusion was done when the cavity is fully annealed at $800\text{ }^{\circ}\text{C}/3\text{hrs}$ and cooldown to desired temperature under UHV conditions before injecting nitrogen into the furnace. While post-doping electropolishing is required to remove coarse nitrides from the surfaces of high-temperature nitrogen doped cavities, no further processing is required for the low-temperature "infusion" recipe showing a clear benefit in reducing processing steps as well as keeping higher gradient with high Q_0 values. In some cases, the increase in accelerating gradient over the baseline was also reported, although the actual mechanism isn't fully understood [10,83,86]. One of the critical requirement for these low temperature recipes is that special cleaning and preparation is needed before loading the cavity into the furnace. The cavity is high pressure rinsed (HPR) and then dried in an ISO 4/5 cleanroom. While in the cleanroom, special caps made from niobium foils were placed to cover the cavity flange openings. The cavity was then transported to the furnace inside a clean, sealed plastic bag. To this date, the recipe was successfully applied to single cell cavities by several research group around world, but no clear advantage was demonstrated in multi cell cavities.

In the quest for high gradient, high quality factor SRF cavities, a two-step low temperature baking process showed an increase in accelerating gradient as well as quality factor well above 40 MV/m [87,88,89] in single cell cavities. Furthermore, the medium temperature baking also showed the improve quality factor with high accelerating gradient [90]. Thus, the continuous research and development towards the high gradient, high quality factor will produce reliable recipe that can be applied to several thousand SRF cavities to be used in future accelerating projects.

VI. Sample Coupon Studies on Doping and Infusion

SRF cavities are much bigger structure and study of sample coupons treated along with SRF cavities provided the useful information about the mechanism behind rf performance on SRF cavities. Several surface sensitive techniques; Scanning electron microscope, Electron diffraction X-ray, Transmission electron microscopy, Secondary ion mass spectroscopy, X-ray photoelectron spectroscopy, Magnetometry and Tunneling.

A. Surface Morphology

Surface imaging with SEMs and also with EDX allowed looking into the surface of niobium after the nitrogen doping. Almost all high temperature doping recipe produces the triangular or star like shaped structures on the surfaces of niobium (Fig. 11). These structures are identified as normal conducting nitride, mainly $\beta\text{-Nb}_2\text{N}$ [45], which are removed using electropolishing in order to achieve the high Q_0 in SRF cavities. It was found that the density and size of the normal conducting niobium nitrides depends on the temperature, duration of nitrogen doping and grain orientation of niobium [91].

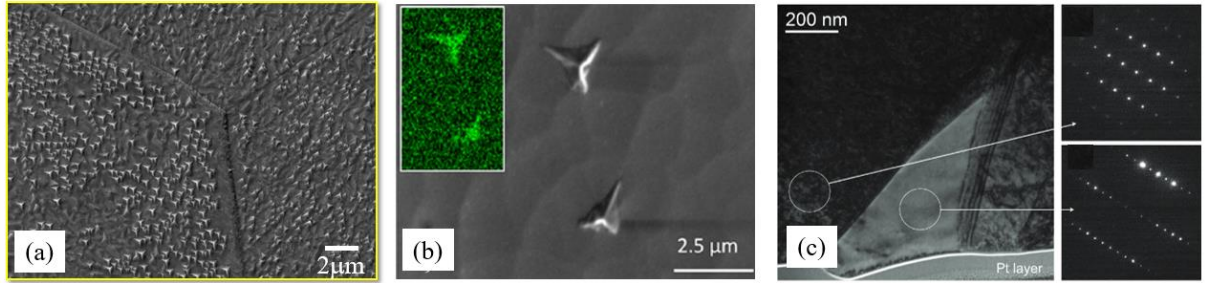


Figure 11. (a) SEM image of nitrogen doped (2N6) Nb sample at 800 °C (Dhakal 2019), (b) SEM and EDX image (inset) elemental map for NK_α of nitrogen doped (20N30) sample at 800 °C [45] and (c) TEM image of Nb sample of nitrogen doped (20N0) at 800 °C with nano electron diffraction image of Nb, [113] zone axis (upper) and of Nb_2N close to [310] zone axis (lower) [44].

A. Secondary ion mass spectroscopy (SIMS)

SIMS has been an excellent tool in order to measure the elemental concentration on the surface of the nitrogen doped Nb samples. Ions beams, primarily $^{16}\text{O}_2^+$, $^{16}\text{O}^-$, $^{133}\text{Cs}^+$ or B_n^{m+} ($n=1-5$, $m=1,2$) are used to bombard on the sample surface at an energy that is enough to eject secondary ions from the surface of the Nb. The ejected ions are detected and analyzed by the mass spectrometers to infer the composition of the sample [92]. Concentration of nitrogen as a function

of depth profiles and other impurities such as oxygen, hydrogen, carbon dioxides, and carbon monoxides are typically measured during the SIMS study depending on the detection limit of the instrumentation. It is to be remembered that the quality factor of SRF cavities depends on the elemental compositions (impurities) within the rf penetration depth. The additional rf losses can be anticipated due to the large segregation of impurities even deeper than the rf penetration, since those sites acts as the effective pinning centers for the residual magnetic field and thereby contributing to the vortex related rf loss [93]. The concentration profiles measured on nitrogen doping seems to follow the simulation results using Fick's laws [42]. As expected, the variation on nitrogen concentration is observed depending on the nitrogen partial pressure [43], temperature of diffusion [50], and duration of nitrogen doping [61] as shown in Fig. 12.

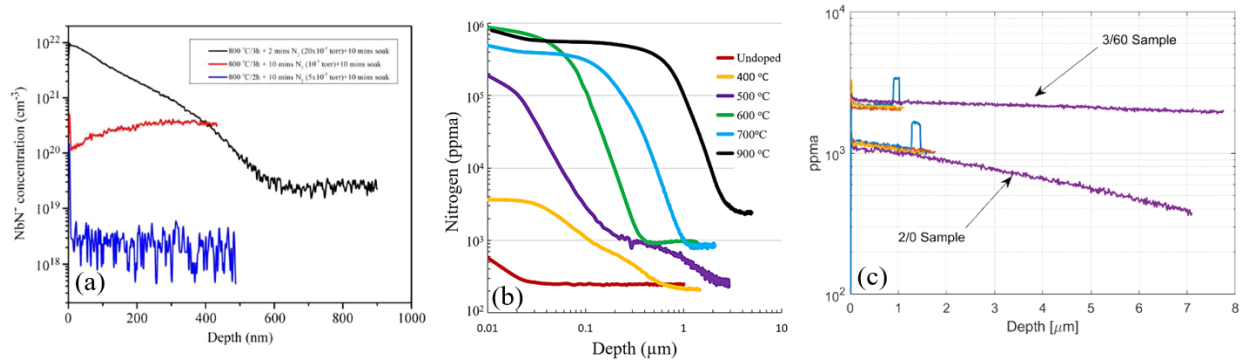


Figure 12. Diffusion depth profile of nitrogen with respect to the (a) partial pressure of nitrogen [43], (b) diffusion temperature [50] and (c) duration of time [61].

SIMS measurements were also carried out samples treated in nitrogen environments at low temperatures and also with titanium doped samples [94]. The diffusion of nitrogen within the rf penetration depth (~50 nm) was observed when the baking temperature was kept 150-200 °C [10,12, 45,95]. Some SIMS measurements suggested the increase concentration of carbon and oxygen is responsible for the increased Q when cavities were heat treated at low temperature [96]. In fact, SIMS studies showed higher concentration of oxygen and carbon as a result of heat treatments above 120 °C [8, 11, 53, 68, 94, 97].

B. X-ray photoelectron spectroscopy (XPS)

XPS studies are done in order to identify the near surface composition on SRF niobium. Historically there has been several XPS studies done in order to understand the loss mechanism of SRF cavities on EP, BCP and Low temperature baked SRF niobium [98,99]. XPS studies on those treatments reveals the complex oxide substructures (Nb_2O_5 , NbO , NbO_2 , $\text{Nb}_x\text{O}_{1-x}$) within the rf penetration depth (~ 10 nm) are highly responsible to the rf performance of SRF cavities (Fig. 13) [12, 45, 53, 69].

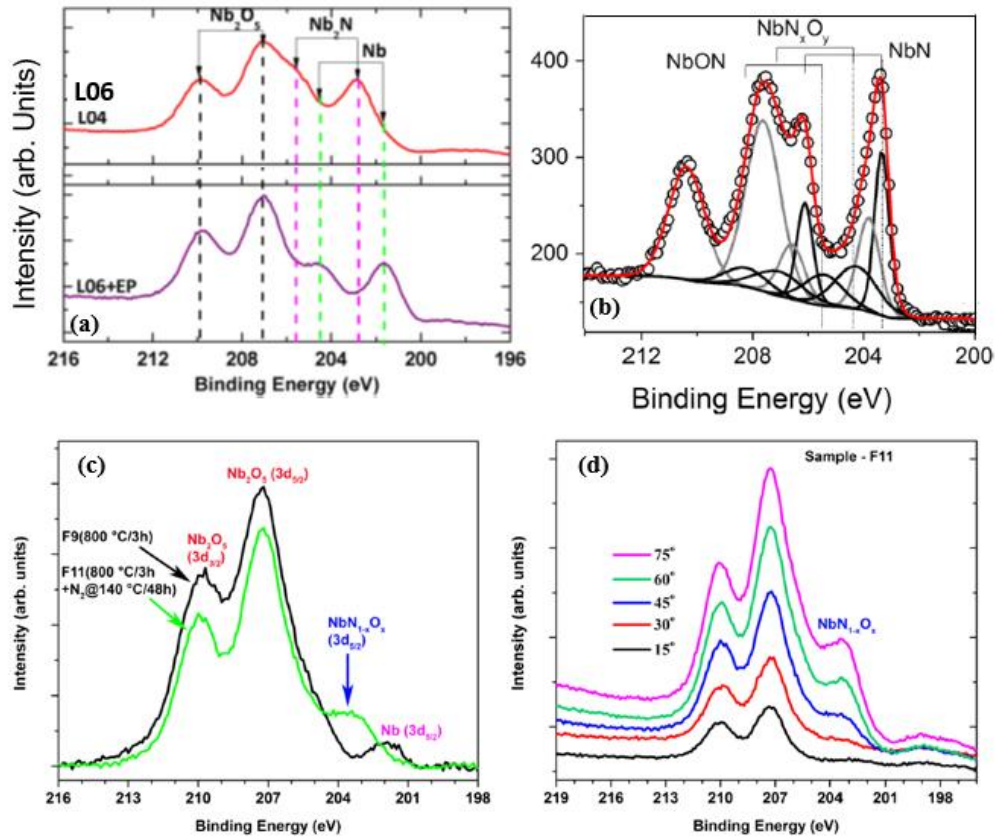


Figure 13. (a) Nb 3d XPS spectra (takeoff angle of 75°) of N-doped (2N6) at 800 °C Nb samples before and after the ~ 6 μm surface removal with EP [53]. (b) Deconvoluted Nb 3d lines measured for the Nb samples after nitridation at 800 °C [45]. (c) Background subtracted XPS spectra on sample F9 (800 °C/3 hrs, no doping) and F11 (800 °C=3 hrs +140 °C/48 hrs at 25 mTorr N_2) at 45° takeoff angle. And, (d) Angle resolved XPS on sample F11 (low temperature nitrogen infusion sample) [12].

C. Magnetometry

The superconducting properties such as the transition temperature and critical fields can be extracted from the dc magnetization and susceptibility measurements. In particular, dc magnetization can be used to estimate the field of first flux penetration (H_{fp}), which is believed to be one of the cause of cavity quench. The measurement showed that H_{fp} is lowered by $\sim 15\%$ due to the nitrogen doping (Fig. 14) [100, 101,102] with no significant change in the bulk superconducting properties, confirming that the doping volume is smaller compared to the sample size.

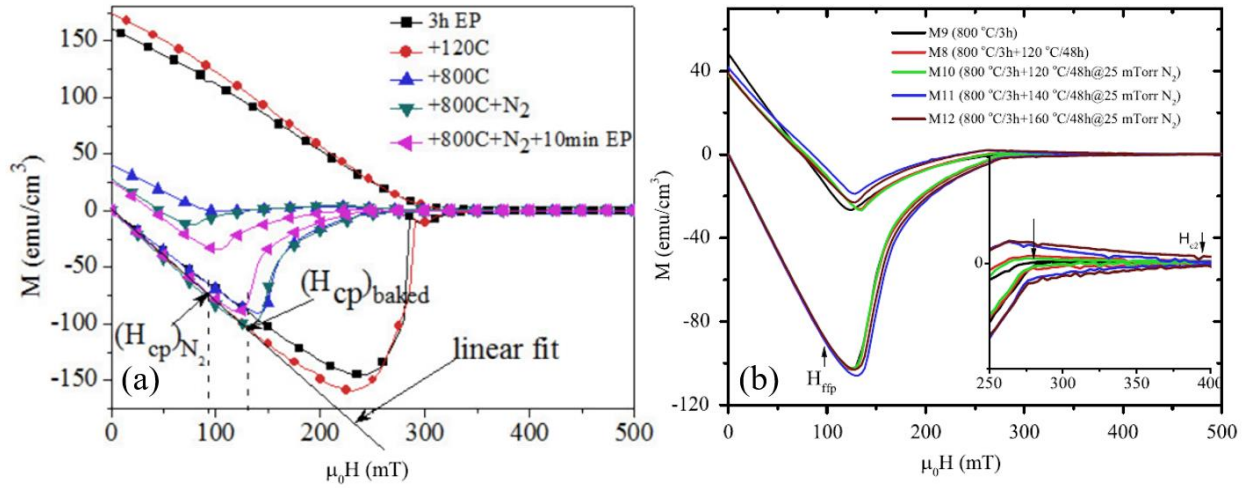


Figure 14. Isothermal dc magnetic hysteresis of samples (a) several surface treatments including nitrogen doped and followed by EP [101]. (b) Sample with nitrogen infusion at low temperature [12]. About 15% reduction in first flux penetration was observed after nitrogen doped samples, whereas no significant change in H_{fp} was observed in low temperature nitrogen infused samples.

The ac susceptibility measurement technique has been used to study the pinning and vortex motions in many superconductors. The real part of the susceptibility is the result of the diamagnetic shielding of the magnetic field whereas the imaginary parts give the information about the loss mechanism. The external magnetic field dependence of ac susceptibility can be used to extract the surface critical fields H_{c1} and H_{c2} . In some geometrical condition, when the external magnetic field is parallel to the sample, the nucleation of the superconducting phase in a thin surface sheath was first discovered by Saint-James and de Gennes [103] up to surface critical field H_{c3} . The ratio H_{c3}/H_{c2} was estimated to be ~ 1.7 using Ginzburg-Landau theory. It has been previously reported

that the experimentally measured ratio is higher than theoretical number for several Nb samples [104, 105] and the ratio increases with decreasing the electronic mean free path. The ratio for nitrogen doped niobium was found to be closer to the theoretical limit [100,101], even though, the electronic mean free path was assumed to be low due to the nitrogen diffusion in to the Nb surface.

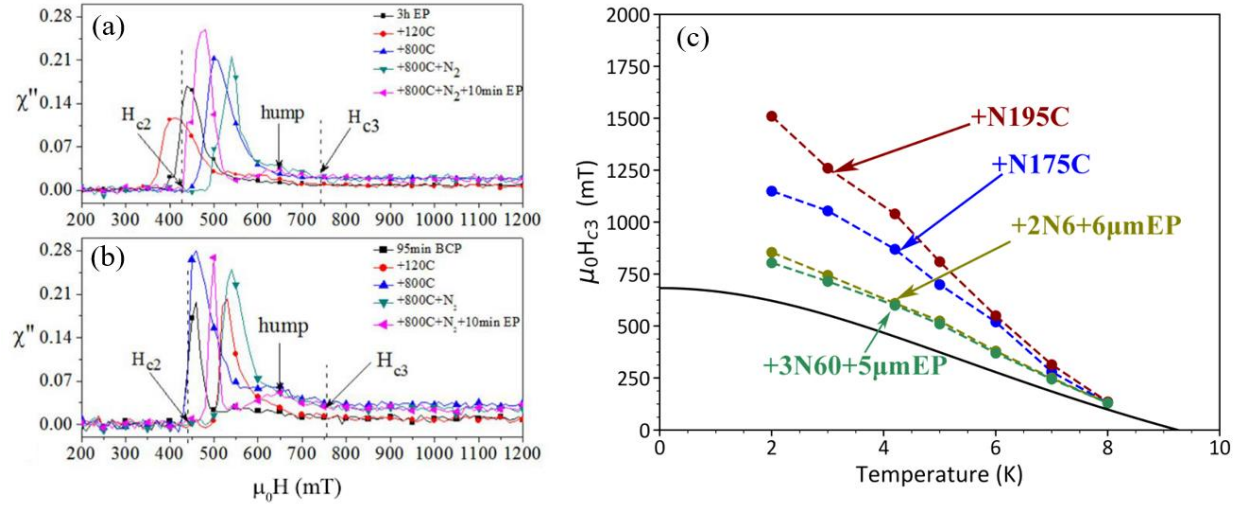


Figure 15. Imaginary part, χ'' , of dc magnetic field-swept-mode ac susceptibilities of nitrogen doped sample with initial surface (a) EP, (b) BCP, followed by EP [101]. And (c) the surface critical field of clean Nb (solid line), nitrogen doped Nb followed by EP and low temperature nitrogen infused Nb samples [106].

D. Tunneling Measurements

The BCS surface resistance depends on many superconducting parameters and among them are the superconducting gap and density of states (DOS) of the quasi-particles at the Fermi level. The tunneling spectroscopy such as point contact tunneling (PCT) and scanning tunneling microscope (STM) are particularly useful in determining the DOS of quasi-particles, superconducting gaps, local distribution of the DOS and gaps as well as imaging vortices. PCT measurements done on nitrogen doped Nb showed the homogeneous distribution of the superconducting gap compared to non-doped samples and also the better surface oxidation states on surface [107]. The oxide structures is particularly beneficial in reducing the loss related to the two level system [108]. Recent STM measurements on cut out samples from nitrogen doped cavities showed the homogeneity of the superconducting gap with broadening of DOS [109] predicted for the dirty superconductors [110]. Furthermore, the vortex imaging with STM showed

the slightly reduced but homogenous superconducting gap and lower coherence length compared to the traditionally prepared niobium cavities.

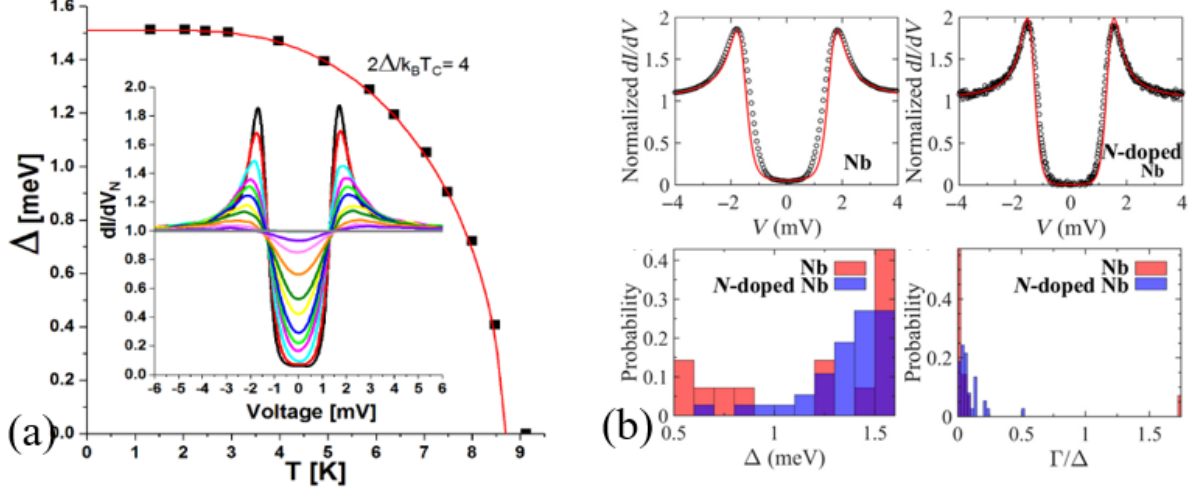


Figure 16. (a) Temperature dependence of Δ for typical tunnel junction measured using point contact tunneling (PCT) shown in the insert [107]. (b) Scanning tunneling spectrum (dots) and BCS-Dynes fit (red line) acquired on Nb and N-doped Nb cavity cutout samples, respectively, at $T=1.5$ K [109].

VII. Theoretical Models

As mentioned earlier, the increase in quality factor can be realized by minimizing the surface resistance, either residual or BCS or both residual and BCS resistance. Statistically, it is found that the residual resistance of doped SRF cavities is lower than non-doped counterpart tested in the low residual magnetic field environment. It is to be noted that the residual magnetic field has a severe effect on doped cavities compared to non-doped cavities [66,111, 112, 113]. Historically, it is believed that the hydrogen in niobium is responsible for higher residual resistance due to the precipitation of hydrogen forming normal conducting hydrides within the rf penetration depth [114,115,116,117]. Some improvement in quality factor at low accelerating gradient and a significant improvement in quality factor with increased accelerating gradient was observed when cavities were baked at low temperature. Even though no unanimous theory or model exist at this time, several evidence shows that the impurities (O and H) as well as their interactions with vacancies play a role in order to minimize the rf loss in SRF cavities due to low temperature baking [118,119,120,121,122]. The presence of nitrogen (or even titanium) traps the hydrogen, preventing

the formation of lossy hydrides [123,124,125, 126, 127,128] probably leading to the lower residual resistance in doped SRF cavities .

One of the peculiar observations in doped cavity is the increase in quality factor as a function of the microwave field tangential to the inner surface of cavity. This means that the surface resistance decreases with the rf field, contrary to perception that the microwave field suppressed the superconductivity leading to the decrease in quality factor Q_0 with accelerating gradient $E_{acc} \propto H_{rf}$ [129]. The quality factor of doped SRF cavities increase with the increase in rf field up to $H_{rf} \sim 100$ mT and is then limited by either quenched or by high field Q -slope, typically observed in non-doped BCP or EP cavities.

The original BCS theory was developed without taking in to account of the amplitude of rf field and this theory explains well the temperature dependence of surface resistance at low rf field [130,131]. The theory was extended to explain the high field Q -slope in SRF cavities, which may be related to the non-linear BCS resistance [132,133]. Soon after the first demonstration of Q -rise phenomena after the titanium doping in SRF cavities [8], the BCS theory was extended taking into account of the moving Cooper pairs in the presence of rf field cavities [134]. The calculation reproduced the rf field dependence surface resistance of titanium doped cavity and consequently the nitrogen doped cavities [135].

Gurevich [110] proposed that microwave suppression of surface resistance comes from the current-induced broadening of the quasiparticle density of states. The BCS surface resistance takes the logarithmic dependence with the microwave field in dirty limit, as experimentally observed in Ti [136] and nitrogen doped cavity [51,137,138, 139]. The microwave suppression of surface resistance was also previously observed in thin films and explained due to the non-equilibrium quasi-particle distribution function leading to the enhancement in supercurrent [140]. A theoretical model in which the surface resistance of a superconductor coated with a thin normal metal was recently presented and showed that the $R_s(B_p)$ behavior observed in SRF cavities following different surface preparations can be explained with changes in the thickness of the normal layer and of the interface boundary resistance [141]. A recent theoretical model proposed by Gurevich extends the zero-field BCS surface resistance to high rf fields, in the dirty limit [142]. Such a model calculates $R_s(H)$ from the nonlinear quasiparticle conductivity $\sigma_1(H)$, which requires knowledge of the quasiparticles' distribution function. The calculation was done for two cases, one which assumes the equilibrium Fermi-Dirac distribution function and one for a non-

equilibrium frozen density of quasiparticles. A non-equilibrium distribution function is appropriate when the rf period is shorter than the quasiparticles' relaxation time. $R_s(H)$ is calculated numerically for these two cases and it depends on a single parameter, α , which is related to the heat transfer across the cavity wall, the Nb-He interface and between quasiparticles and phonons. The theory explained well the microwave surface resistance in cavities with low temperature nitrogen infusion cavities [12].

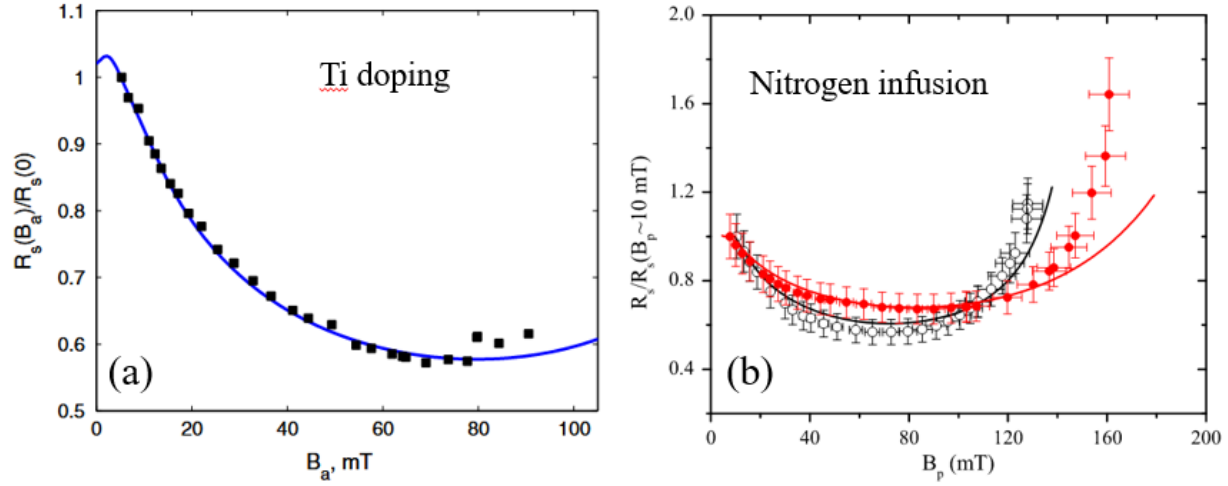


Figure 17. Normalized surface resistance as a function of peak surface magnetic field on cavity surface (a) Ti-doped cavity [110] and (b) Nitrogen infused srf cavities [12], the solid lines are calculated using the model described in ref. [142].

Several other models are reported in order to understand the microwave resistance in SRF cavities extending the theory to clean, dirty, equilibrium and non-equilibrium superconductors [143,144,145, 146,147]. The nitrogen doping and infusion studies were also extended to different frequency cavities [148,149], showing that the frequency might play the role in the field dependence of microwave surface resistance [146]. In addition, two-fluid models taking into account the surface impurities on SRF cavities were extended in order to fit the field dependent surface resistance in order to extract the superconducting parameters responsible for the reduced rf loss in doped SRF cavities [150,151].

VIII. Summary and Future Outlook

Engineering the concentration of nitrogen within the rf penetration depth in SRF cavities have been extremely beneficial in order to achieve the high quality factor, potentially cost saving on current and future SRF based accelerators. SRF cavities with high quality factor ($Q_0 > 3 \times 10^{10}$) at 2.0 K in accelerating gradient ~ 25 MV/m has been successfully produced commercially and is in process of installation in LCLS-II. Efforts are being made in order to extend the high quality factors towards higher accelerating gradient with modification of existing recipe as well as exploring the new recipes. High Q_0 and high gradient SRF cavities would be of great interest for lowering the cryogenic heat load of future high-energy accelerators.

High quality factor SRF cavities are also drawing interest in several other applications. For example, the quantum computing with microwave resonators [152,153,154] and axion dark matter research [155]. Extremely high quality factor with decay time of the order of few seconds were measured in SRF cavities in quantum temperature limit [156]. In addition to Nb cavities, the alternative materials Nb₃Sn are being explored in order to achieve high quality factor, however so far the accelerating gradient are limited to below 20 MV/m [157,158,159]. Thin Nb₃Sn cavities are fabricated using thermal diffusion of Sn on Nb cavities, potential for industrial applications [160]. For high accelerating gradient cavities, multilayers of superconducting are being considered [161,162].

IX. Acknowledgements

We would like to acknowledge Dr. G. Ciovati, Dr. R. Geng and Dr. A. Palczewski from Jefferson Lab for helpful discussions. We would like to acknowledge Dr. S. Balachandran from Applied Superconductivity Center, NHMFL with fruitful discussions. This manuscript has been authored by Jefferson Science Associates, LLC under U.S. DOE Contract No. DE-AC05-06OR23177.

References

1. Accelerator for American, <http://www.acceleratorsamerica.org/index.html>.
2. C. E. Reece and G. Ciovati, Superconducting RF technology R&D for future accelerator Applications, *Rev. of Accel. Sci. and Technol.*, **5**, 285-312 (2012).
3. H. Padamsee, Future prospects of superconducting RF for accelerator applications, *Rev. of Accel. Sci. and Technol.*, **10**, 125-156 (2019).
4. H. Padamsee, History of gradient advances in SRF, arXiv: 2004.06720 (2020).
5. J. Bardeen, L. N. Cooper, and J. R. Schrieffer, Theory of superconductivity, *Phys. Rev.* **108**, 1175 (1957).
6. D. C. Mattis and J. Bardeen, Theory of the anomalous skin effect in normal and superconducting metals, *Phys. Rev.* **111**, 412 (1958).
7. P. Dhakal, G. Ciovati, and G. R. Myneni, A path to higher Q_0 with large grain niobium cavities, in *Proc. of IPAC 2012*, New Orleans, USA (2012). www.jacow.org.
8. P. Dhakal, *et al.*, Effect of high temperature heat treatments on the quality factor of a large-grain superconducting radio-frequency niobium cavity, *Phys. Rev. ST Accel. Beams* **16**, 042001. (2013).
9. A. Grassellino *et al.*, Nitrogen and argon doping of niobium for superconducting radio frequency cavities: a pathway to highly efficient accelerating structures, *Supercond. Sci. Technol.* **26**, 102001 (2013).
10. A. Grassellino *et al.*, Unprecedented quality factors at accelerating gradients up to 45 MVm⁻¹ in niobium superconducting resonators via low temperature nitrogen infusion, *Supercond. Sci. Technol.* **30**, 094004 (2017).
11. P.N. Koufalas, F. Furuta, M. Ge, D. Gonnella, J.J. Kaufman, M. Liepe, J.T. Maniscalco, R.D. Porter, Low temperature nitrogen baking of a Q_0 SRF cavities, In *Proc. of LINAC2016, East Lansing MI, USA*, (2016). www.jacow.org.
12. P. Dhakal, S. Chetri, S. Balachandran, P. J. Lee, and G. Ciovati, Effect of low temperature baking in nitrogen on the performance of a niobium superconducting radio frequency cavity, *Phys. Rev. Accel. Beams* **21** 032001 (2018).
13. R. L. Geng, H. Hayano, H. Ito, Y. Fuwa, Y. Iwashita, Z. Li, Performance of first prototype multi-cell low-surface-field shape cavity, in *Proc. of SRF2019*, Dresden, Germany (2019). www.jacow.org.
14. www.jacow.org
15. R. Ballantini, A. Dacca, G. Gemme, R. Parodi, and L. Mattera, Improvement of the maximum field of accelerating cavities by dry oxidization, in *Proc. of the 9th Workshop on RF Superconductivity*, Santa Fe, NM (1999). www.jacow.org
16. E. W. Hoyt, Niobium surfaces for RF superconductors, *SLAC Technical Note No. SLAC-PUB-977*, 1971.
17. G. Ciovati, G. Myneni, F. Stevie, P. Maheshwari, and D. Griffis, High field Q slope and the baking effect: Review of recent experimental results and new data on Nb heat treatments, *Phys. Rev. ST Accel. Beams* **13**, 022002 (2010).
18. J. Stohr, *Linac Coherent Light Source II (LCLS-II) Conceptual Design Report*. United States: (2011). doi:10.2172/1029479.
19. B. Aune *et al.*, Superconducting TESLA cavities, *Phys. Rev. ST Accel. and Beams* **3**, 092001 (2000).
20. J. N. Galayda, The Linac Coherent Light Source-II project" in *Proc. IPAC2014*, Dresden, Germany, (2014). www.jacow.org
21. M. Liepe *et al.*, The joint high Q_0 R&D program for LCLS-II, in *Proc. 5th Int. Particle Accelerator Conf. (IPAC'14)*, Dresden, Germany (2014). www.jacow.org.
22. C. E. Reece, High-Q development plan and choice of Q , *JLab Tech note* 14-015.
23. P. Bishop *et al.*, LCLS-II SRF cavity processing protocol development and baseline cavity performance demonstration, in *Proc. of SRF2015*, Whistler, BC, Canada (2015). www.jacow.org.
24. M. Ge, R. Eichhorn, B. Elmore, F. Furuta, D. Gonnella, Performance of nitrogen doped 9-cell srf cavities in vertical tests at Cornell university, in *Proc. of SRF2015*, Whistler, BC, Canada (2015). www.jacow.org.
25. A. D. Palczewski, G. Ereemeev, R. L. Geng, and C. E. Reece, Quench studies of high temperature nitrogen doped 9 cell cavities for use in the LCLS-II baseline prototype cryomodule at Jefferson laboratory, in *Proc. of IPAC2015*, Richmond, VA, USA. www.jacow.org.
26. M. Merio, A.C. Crawford, A. Grassellino, A. Rowe, M. Wong, M. Checchin, M. Martinello, Furnace N2 doping treatments at Fermi Lab, In *Proc. of SRF2015*, Whistler, Bc, Canada (2015). www.jacow.org.
27. A. D. Palczewski, R. L. Geng, and C. E. Reece, Analysis of new high- Q_0 srf cavity test by nitrogen gas doping at Jefferson lab, in *Proc. of LINAC2014*, Geneva, Switzerland (2014). www.jacow.org.

-
28. F. Furuta, B. Bullock, R. Eichhorn, A. Ganshin, M. Ge, G. Hoffstaetter, J. Kaufman, M. Liepe, J. Sears, TM Furnace qualification at Cornell, in *Proc. of SRF2013*, Paris, France (2013). www.jacow.org.
 29. TM Vacuum Products Inc, <http://www.tmvacuum.com>.
 30. K. Umemori, *et al.*, Vertical test results of nitrogen doped srf cavities at KEK, in *Proc. of IPAC2016*, Busan, Korea (2016). www.jacow.org.
 31. T. Okada *et al.*, Improvement of cavity performance by nitrogen doping at KEK, in *Proc. of LINAC2018*, Beijing, China (2018). www.jacow.org.
 32. C. Benvenuti, L. Chiggiato, L. Parrini, R. Russo, Reactive diffusion produced niobium nitride films for superconducting cavity applications, *Nucl. Instrum. Methods Phys. Res. A Accel. Spectrom. Detect. Assoc. Equip.*, **336**, 16-22 (1993).
 33. R. Musenich, P. Fabbriatore, G. Gemme, R. Parodi, M. Viviani, B. Zhang, Growth of niobium nitrides by nitrogen-niobium reaction at high temperature, *J. of Alloys and Compounds* **209**, 319 (1994).
 34. Y. Ufuktepe, A. H. Farha, S. Kimura, T. Hajiri, F. Karadağ, M. A. Al Mamun, A. A. Elmustafa, G. Myneni, and H. E. Elsayed-Ali, Structural, electronic, and mechanical proper-ties of niobium nitride prepared by thermal diffusion in nitrogen, *Mater. Chem. Phys.* **141**, 393 (2013).
 35. W. Mayr, W. Lengauer, V. Buscaglia, J. Bauer, M. Bohn, and M. Fialin, Nitridation of Ti/Nb alloys and solid-state properties of δ -(Ti,Nb)N, *J. of Alloys and Compounds* **262**, 521 (1997).
 36. N. Cansever, M. Danişman, and K. Kazmanli, The effect of nitrogen pressure on cathodic arc deposited NbN thin films, *Surface and Coatings Technology* **202**, 5919 (2008).
 37. C. Y. Ang, Activation energies and diffusion coefficients of oxygen and nitrogen in niobium and tantalum, : *Acta Metall.* **1**, 123–125 (1953).
 38. J. Keinonen, J. Raisanen, and A. Anttila, Diffusion of nitrogen in vanadium and niobium, *Appl. Phys. A, Materials Science & Processing*, **34**, 49-56 (1984).
 39. T. Ogurtani and E. M. Uygur, Diffusion of Nitrogen in Niobium with Special Reference to Temperature Dependence of the Activation Energy, *Trans. Japan Inst. of Metals*, **13**(6), 396, (1972).
 40. C. J. Clenny and C. R. Rosa, Nitridation kinetics of niobium in the temperature range of 873 to 1273 K, *Met. Trans. A* **11**, 1385 (1980).
 41. A. D. Palczewski, C. E. Reece, M.J. Kelly, J. Tuggle, Investigation of nitrogen absorption rate and nitride growth on SRF cavity grade RRR niobium as a function of furnace temperature, in *Proc. of LINAC2016*, East Lansing, MI, USA (2018).
 42. D. Gonnella, R.G. Eichhorn, F. Furuta, G. M. Ge, T. Gruber, G. H. Hoffstaetter, J. J. Kaufman, P. N. Koufalis, M. Liepe, J.T. Maniscalco, Improved N-doping protocols for SRF cavities, in *Proc. of IPAC2016*, Busan, Korea (2016). www.jacow.org.
 43. P. Dhakal, G. Ciovati, P. Kneisel, and G. R. Myneni, Enhancement in quality factor of SRF niobium cavities by material diffusion, *IEEE Transactions on Applied Superconductivity* **25**, 1 (2014).
 44. Y. Trenikhina, A. Grassellino, O. S. Melnychuk, A. Romanenko, Characterization of nitrogen doping recipes for the Nb SRF cavities, in *Proc. of SRF2015*, Whistler, BA, Canada (2015). www.jacow.org
 45. A. Dangwal Pandey, G. Dalla Lana Semione, A. Prudnikava, T. F. Keller, H. Noei, V. Vonk, Y. Tamashevich, E. Elsen, B. Foster, and A. Stierle, Surface characterization of nitrogen-doped Nb (100) large-grain superconducting RF cavity material, *J. Mater. Sci.* **53**, 10411 (2018).
 46. Z. Yang, X. Lu, W. Tan, J. Zhao, D. Yang, Y. Yang, Y. He, K. Zhou, XPS studies of nitrogen doping niobium used for accelerator applications, *Appl. Surface Science* **439**, 1119 (2018).
 47. G. Brauer, Nitrides, cabonitrides and oxynitrides of niobium, *J. of Less Com. Met.* **2**, 131 (1960).
 48. W. M. Albrecht and W. D. Goode, Reaction of nitrogen with niobium, BMI 1360 (1959).
 49. J. K. Spradlin, A. D. Palczewski, H. Tian and C. E. Reece, Analysis of surface nitrides created during doping heat treatments of niobium, in *Proc. of the SRF 19 Dresden Germany*, (2019). www.jacow.org.
 50. J. Tuggle, U. Pudasaini, F. A. Stevie, M. J. Kelley, A. D. Palczewski, and C. E. Reece, Secondary ion mass spectrometry for superconducting radiofrequency cavity materials, *J. Vac. Sci. Technol.* **B36**, 052907 (2018).
 51. P. Dhakal, J. Makita, G. Ciovati, P. Kneisel, and G. R. Myneni, Nitrogen doping study in ingot niobium cavities, in *Proc. of IPAC2015*, Richmond, VA, USA (2015). www.jacow.org.
 52. J. Makita, P. Dhakal, and G. Ciovati, Temperature mapping of nitrogen doped niobium superconducting radio frequency cavities, in *Proc. of IPAC2015*, Richmond, VA, USA (2015). www.jacow.org.
 53. P. Dhakal, S. Chetri, S. Balachandran, U. Pudasaini, P. J. Lee, and G. Ciovati, Surface characterization of nitrogen-doped high purity niobium coupons compared with superconducting rf cavity performance, *Phys. Rev. Accel. Beams* **22**, 122002 (2019).

-
54. M. P. Kelly, and T. Reid, Surface processing for bulk niobium superconducting radio frequency cavities, *Supercond. Sci. Technol.* **30**, 043001 (2017).
 55. H. Tian, C. E. Reece, M. J. Kelley, S. Wang, L. Plucinski, K. E. Smith, and M. M. Nowell, Surface studies of niobium chemically polished under conditions for superconducting radio frequency (SRF) cavity production, *Appl. Surf. Sci.* **253**, 1236 (2006).
 56. C. E. Reece, A. C. Crawford and R. L. Geng, Improved performance of JLAB 7-cell cavities by electropolishing, in *Proc. of PAC2009*, Vancouver, BC, Canada (2009). www.jacow.org.
 57. F. Marhauser, J. Follkie, C. E. Reece, Investigation of differential surface removal due to electropolishing at JLAB, in *Proc. of IPAC2015*, Richmond, VA USA (2015). www.jacow.org.
 58. A. C. Crawford, Extreme diffusion limited electropolishing of niobium radiofrequency cavities, *Nucl. Instrum. Methods Phys. Res., Sect. A* **849**, 5 (2017).
 59. C. E. Reece, F. Marhauser, and A. D. Palczewski, The transfer of improved cavity processing protocols to industry for LCLS-II: N-doping and electropolishing, in *Proc. of SRF2015*, Whistler, BC, Canada (2015). www.jacow.org.
 60. W. Singer, X. Singer, A. Brinkmann, J. Iversen, A. Matheisen, A. Navitski, Y. Tamashevich, P. Michelato, and L. Monaco, Superconducting cavity material for the European XFEL, *Supercond. Sci. Technol.* **28**, 085014 (2015).
 61. D. Gonnella *et al.*, Industrial cavity production: Lessons learned to push the boundaries of nitrogen-doping, in *Proc. of SRF2019*, Dresden, Germany (2019). www.jacow.org
 62. D. Gonnella, Statistical analysis of nitrogen-doped cavity production for LCLS-II, in *presentation TTC 2020*, Geneva, Switzerland (2020).
 63. A. Romanenko, A. Grassellino, O. Melnychuk, and D. A. Sergatskov, Dependence of the residual surface resistance of superconducting radio frequency cavities on the cooling dynamics around T_c , *J. Appl. Phys.* **115**, 184903 (2014).
 64. D. Gonnella *et al.*, Nitrogen-doped 9-cell cavity performance in a test cryomodule for LCLS-II, *J. Appl. Phys.* **117**, 023908 (2015).
 65. T. Kubo, Flux trapping in superconducting accelerating cavities during cooling down with a spatial temperature gradient, *Prog. Theor. Exp. Phys.* 053G01 (2016).
 66. P. Dhakal, G. Ciovati, and A. Gurevich, Flux expulsion in niobium superconducting radio-frequency cavities of different purity and essential contributions to the flux sensitivity, *Phys. Rev. Accel. Beams* **23**, 023102 (2020)
 67. A. D. Palczewski, O. S. Melnychuk, D. A. Sergatskov, and D. Gonnella, Study of flux trapping variability between batches of Tokyo Denka niobium used for the LCLS project and subsequent 9-cell RF loss distribution between the batches, in *Proc. of SRF2019*, Dresden, Germany (2019). www.jacow.org.
 68. T. Konomi, T. Dohmae, Y. Hori, E. Kakopresenter, T. Kubo, G.-T. Park, H. Sakai, K. Umemori, J. Kamiya, K. Takeishi, T. Nagata, Trial of nitrogen infusion and nitrogen doping by using J-PARC furnace, in *Proc. of SRF2017*, Lanzhou, China (2017). www.jacow.org.
 69. P. Sha, J. P. Dai, and F. Jiao, Research of nitrogen doping in IHEP, in *Proc. of IPAC2016*, Busan, Korea (2016). www.jacow.org.
 70. S. Chen, J.-K. Hao, L. Lin *et al.*, Successful nitrogen doping of 1.3GHz single cell superconducting radio-frequency cavities, *Chin. Phys. Lett.* **35** 037401 (2018).
 71. S. Chen, M. Chen, L. W. Feng, J. K. Hao, L. Lin, K. X. Liu, S. W. Quan, F. Wang, F. Zhu, Nitrogen doping studies of superconducting cavities at Peking University, in *Proc. of SRF2019*, Dresden, Germany (2019). www.jacow.org.
 72. W. Singer *et al.*, Production of superconducting 1.3-GHz cavities for the European X-ray free electron laser, *Phys. Rev. Accel. Beams* **19**, 092001 (2016).
 73. D. Reschke, Performance of superconducting cavities for the European XFEL, in *Proc. of IPAC2016*, Busan, Korea (2016). www.jacow.org.
 74. L. Evans and S. Michizano, The international linear collider machine staging report 2017, arXiv:1711.00568.
 75. A. D. Palczewski, Development of a qualitative model for N-doping effects on Nb SRF cavities, in *presentation of SRF2019*, Dresden, Germany (2019). paper TUFUA3.
 76. D. Gonnella, The LCLS-II HE high Q and gradient R&D program, in *Proc. of SRF2019*, Dresden, Germany (2019). www.jacow.org.
 77. D. Bafia, A. Grassellino, A. Romanenko, M. Checchin, O. S. Melnychuk, D. A. Sergatskov, J. Zasadzinski, New Insights on Nitrogen Doping, in *Proc. of SRF2019*, Dresden, Germany (2019). www.jacow.org.
 78. M. Ge, P. N. Koufalas, G. Kulina, M. Liepe, J. T. Maniscalco, Low-temperature baking and infusion studies for high-gradient ILC SRF cavities, in *Proc. of LINAC2018*, Beijing, China (2018). www.jacow.org.
 79. T. Konomi *et al.*, Trial of nitrogen infusion and nitrogen doping by using J-PARC furnace, in *Proc. of SRF2017*, Lanzhou, China (2017). www.jacow.org.

-
80. K. Umemori *et al.*, Study on nitrogen infusion for 1.3 GHz SRF cavities using J-PARC furnace, in *Proc. of LINAC2018*, Beijing, China (2018). www.jacow.org.
 81. K. Umemori, E. Kako, T. Konomi, S. Michizono, H. Sakai, J. Tamura, and T. Okada, Study on nitrogen infusion using KEK new furnace, in *Proc. of SRF 2019*, Dresden, Germany (2019). www.jacow.org.
 82. M. Wenskat, A. Prudnikava, D. Reschke, and J. Schaffran, Nitrogen Infusion R&D on single cell cavities at DESY, in *Proc. of SRF2017*, Lanzhou, China (2017). www.jacow.org.
 83. P. Dhakal, Recent development on nitrogen infusion work towards high Q and high gradient, in *Proc. of SRF2019*, Dresden, Germany (2019). www.jacow.org.
 84. G. D. L. Semione, A. Dangwal Pandey, S. Tober, J. Pfrommer, A. Poulain, J. Drnec, G. Schütz, T. F. Keller, H. Noei, V. Vonk, B. Foster, and A. Stierle, Niobium near-surface composition during nitrogen infusion relevant for superconducting radio-frequency cavities, *Phys. Rev. Accel. Beams* **22**, 103102 (2019).
 85. A. Bose, P. Mondal, G. M. Bhalerao, S. V. Kokil, S. Raghavendra, S. C. Joshi, A. K. Srivastava, R. Tewari, Evolution of surface oxides and impurities in high vacuum heat treated Nb: A TEM and TOF-SIMS in-situ study, mechanism and repercussions on SRF cavity applications, *Applied Surface Science* **510**, 145464 (2020).
 86. K. Umemori, New results of KEK N-infusion and mid-T bake, in *presentation at TTC meeting 4-7 Feb 2020*, CERN Switzerland, (2020).
 87. A. Grassellino *et al.*, Accelerating fields up to 49 MV/m in TESLA-shape superconducting RF niobium cavities via 75C vacuum bake” arXiv:1806.09824, (2018).
 88. M. Wenskat *et al.*, A Cross-Lab Qualification of Modified 120 C Baked Cavities, in *Proc. of SRF2019*, Dresden, Germany (2019). www.jacow.org.
 89. D. Bafia, A. Grassellino, Z. Sung, A. Romanenko, O. S. Melnychuk, and J. F. Zasadzinski, Gradient of 50 MV/m in TESLA shaped cavities via modified low temperature bake, in *Proc. of SRF2019*, Dresden, Germany (2019). www.jacow.org.
 90. S. Posen, A. Romanenko, A. Grassellino, O.S. Melnychuk, and D.A. Sergatskov, Ultralow surface resistance via vacuum heat treatment of superconducting radiofrequency cavities, *Phys. Rev. Applied* **13**, 014024 (2020).
 91. J. K. Spradlin, A. D. Palczewski, H. Tian, and C. E. Reece, Analysis of surface nitrides created during doping heat treatments of niobium, in *Proc. of SRF2019*, Dresden, Germany (2019). www.jacow.org.
 92. R. G. Wilson, F. A. Stevie, and C. W. Magee, *Secondary Ion Mass Spectrometry: A Practical Handbook for Depth Profiling and Bulk Impurity Analysis*, John Wiley & Sons, New York, 1989.
 93. G. Ciovati and A. Gurevich, Evidence of high-field radio-frequency hot spots due to trapped vortices in niobium cavities, *Phys.Rev.ST Accel. Beams* **11**, 122001 (2008).
 94. P. Maheshwari, F. A. Stevie, G. R. Myneni, G. Ciovati, J. M. Rigsbee, P. Dhakal, and D. P. Griffis, SIMS analysis of high-performance accelerator niobium, *Surf. Interface Anal.* **46**, 288 (2014)
 95. C. Bate *et al.*, Nitrogen Infusion sample R&D at DESY, in *Proc. of SRF2019*, Dresden, Germany (2019). www.jacow.org.
 96. P. N. Koufalas, J. T. Maniscalco, M. Ge, and M. Liepe, Effect of low temperature infusion heat treatments and 2/0 doping on superconducting cavity performance, in *Proc. of SRF2019*, Dresden, Germany (2019). www.jacow.org.
 97. A.S. Romanenko, A. Grassellino, M. Martinello, Y. Trenikhina, D. Bafia, First direct imaging and profiling TOF-SIMS studies on cutouts from cavities prepared by state-of-the-art treatments, in *Proc. of SRF2019*, Dresden, Germany (2019). www.jacow.org.
 98. H. Tian, C. E.Reece, M. J.Kelley, S. Wang, L. Plucinski, K. E.Smith, M. M.Nowell, Surface studies of niobium chemically polished under conditions for superconducting radio frequency (SRF) cavity production, *Applied Surface Science* **253**, 1236 (2006).
 99. N. Singh, M. N. Deo, M. Nand, S. N. Jha, and S. B. Roy, Raman and photoelectron spectroscopic investigation of high-purity niobium materials: Oxides, hydrides, and hydrocarbons, *J. Appl. Phys.* **120**, 114902 (2016).
 100. A. Vostrikov, Y.-K. Kim, A. Grassellino, A. Romanenko, Modifications of superconducting properties of niobium caused by nitrogen doping recipes for high Q cavities, in *Proc. of IPAC2015*, Richmond, VA USA (2015). www.jacow.org
 101. S. Chetri, D. C. Larbalestier, Z-H. Sung, P. Dhakal, and P. J. Lee, Determination of bulk and surface superconducting properties of N₂-doped cold worked, heat treated and electropolished SRF grade niobium, in *Proc. of SRF2015*, Whistler, BC, Canada (2015). www.jacow.org.
 102. Z. Yang, X. Lu, Y. He, W. Tan, S. Huang, and H. Guo, Magnetic properties and hydrides precipitation observation of nitrogen doping niobium used for accelerator applications, *Results in Physics* **12**, 2155 (2019).
 103. D. Saint-James and P. de Gennes, Onset of superconductivity in decreasing fields, *Phys. Lett.* **7**, **306** (1963).
 104. S. Casalbuoni, E. A. Knabbe, J. Kotzler, L. Lilje, L. von Sawilski, P. Schmuser, and B. Steffen, *Nucl. Instrum. Methods Phys. Res. A* **538**, 45–64 (2005).

105. A. S. Dhavale, P. Dhakal, A. A. Polyanskii, and G. Ciovati, Flux pinning characteristics in cylindrical niobium samples used for superconducting radio frequency cavity fabrication, *Supercond. Sci. Technol.* **25**, 065014 (2012).
106. S. Chetri *et al.*, in preparation.
107. N. R. Groll, G. Ciovati, A. Grassellino, A. Romanenko, J. F. Zasadzinski, T. Proslir, Insight into bulk niobium superconducting RF cavities performances by tunneling spectroscopy, *arXiv:1805.06359* (2018).
108. J. M. Martinis *et al.*, Decoherence in Josephson qubits from dielectric loss, *Phys. Rev. Lett.* **95**, 210503–210506 (2005).
109. E. M. Lechner, B. D. Oli, J. Makita, G. Ciovati, A. Gurevich, and M. Iavarone, Electron tunneling and X-Ray photoelectron spectroscopy studies of the superconducting properties of nitrogen-doped niobium resonator cavities, *Phys. Rev. Applied* **13**, 044044 (2020).
110. A. Gurevich, Reduction of dissipative nonlinear conductivity of superconductors by static and Microwave Magnetic Fields, *Phys. Rev. Lett.* **113**, 087001 (2014).
111. D. Gonnella, J. Kaufman, and M. Liepe, Impact of nitrogen doping of niobium superconducting cavities on the sensitivity of surface resistance to trapped magnetic flux, *J. Appl. Phys.* **119**, 073904 (2016).
112. M. Martinello, A. Grassellino, M. Checchin, A. Romanenko, O. Melnychuk, D. A. Sergatskov, S. Posen, and J. F. Zasadzinski, Effect of interstitial impurities on the field dependent microwave surface resistance of niobium, *Appl. Phys. Lett.* **109**, 062601 (2016).
113. S. Huang, T. Kubo, and R. L. Geng, Dependence of trapped-flux-induced surface resistance of a large-grain Nb superconducting radio-frequency cavity on spatial temperature gradient during cooldown through T_c , *Phys. Rev. Accel. Beams* **19**, 082001 (2016).
114. S. Isagawa, Hydrogen absorption and its effect on low-temperature electric properties of niobium *J. Appl. Phys.* **51**, 4460-4470 (1980).
115. B. Bonin and R. Roth, Q Degradation of niobium cavities due to hydrogen contamination, *Particle Accelerators* **40**, 59-83 (1992).
116. R. E. Ricker and G. R. Myneni, Evaluation of the propensity of niobium to absorb hydrogen during fabrication of superconducting radio frequency cavities for particle accelerators, *J. Res. Natl. Inst. Stand. Technol.* **115**, 353 (2010).
117. D. C. Ford, L. D. Cooley, and D. N. Seidman, First-principles calculations of niobium hydride formation in superconducting radio-frequency cavities, *Supercond. Sci. Technol.* **26**, 095002 (2013).
118. G. Ciovati, Effect of low-temperature baking on the radio-frequency properties of niobium superconducting cavities for particle accelerators, *J. of Appl. Phys.* **96**, 1591 (2004).
119. G. Ciovati, Improved oxygen diffusion model to explain the effect of low-temperature baking on high field losses in niobium superconducting cavities, *Appl. Phys. Lett.* **89**, 022507(2006).
120. B. Visentin, M. F. Barthe, V. Moineau, and P. Desgardin, Involvement of hydrogen-vacancy complexes in the baking effect of niobium cavities. *Phys. Rev. Accel. Beams* **13**, 052002 (2010).
121. A. Romanenko, F. Barkov, L. D. Cooley, and A. Grassellino, Proximity breakdown of hydrides in superconducting niobium cavities. *Supercond. Sci. Technol.* **26**, 035003(2013).
122. M. Wenskat, J. Cizek, M. Oskar Liedke, M. Butterling, C. Bate, P. Hausild, E. Hirschmann, A. Wagner, H. Weise, Vacancy-hydrogen interaction in niobium during low temperature baking, *arXiv:2004.13450* (2020).
123. D. Richter, R. J. Rush, and J. M. Rowe, Localized modes and hydrogen trapping in niobium with substitutional impurities, *Phys. Rev. B, Condens. Matter* **27**, 6227 (1983).
124. G. Pfeifer and H. Wipf, The trapping of hydrogen in niobium by nitrogen interstitials, *J. Phys. F, Metal Phys.* **6**, 167 (1976).
125. P. Garg, S. Balachandran, I. Adlakha, P. J. Lee, T. R. Bieler, and K. N. Solanki, Role of nitrogen on hydride nucleation in pure niobium by first principles calculations, in *Proc. of SRF2017*, Lanzhou, China (2017). www.jacow.org.
126. S. Balachandran, P. J. Lee, S. Chetri, D. C. Larbalestier, and P. Dhakal, Hydrogen distribution and hydride precipitation in SRF Nb revealed by metallographic techniques, *presented at SRF2017*, Lanzhou, China (2017). Paper ID TUXBA05, www.jacow.org.
127. P. Garg, S. Balachandran, I. Adlakha, P. J. Lee, T. R. Bieler, and K. N. Solanki, Revealing the role of nitrogen on hydride nucleation and stability in pure niobium using first-principles calculations, *Supercond. Sci. Technol.* **31**, 115007 (2018).
128. N. Sitaraman, T. Arias, R. G. Farber, S. J. Sibener, R. D. Veit, J. T. Maniscalco, and M. Liepe, Ab initio calculations on impurity doped niobium and niobium surfaces, in *Proc. of SRF2019*, Dresden, Germany (2019). www.jacow.org.

129. B. I. Ivlev, S. G. Lisitsyn, and G.M. Eliashberg, Nonequilibrium excitations in superconductors in high-frequency fields, *J. Low Temp. Phys.* **10**, 449 (1973).
130. J. Halbritter, Comparison between measured and calculated RF losses in the superconducting state, *Zeitschrift für Physik* **238**, 466 (1970)
131. K. Saito and P. Kneisel, Temperature dependence of surface resistance of niobium at 1300 MHz-comparison to BCS theory, in *Proc. of SRF1999*, Santa Fe, New Mexico, USA (1999). www.jacow.org.
132. A. Gurevich, Multiscale mechanisms of SRF breakdown, *Physica C* **441**, 38 (2006).
133. P. Bauer, N. Solyak, G. Ciovati, G. Ereemeev, A. Gurevich, L. Lilje, and B. Visentin, Evidence of non-linear BCS resistance in SRF cavities, *Physica C* **441** 51 (2006).
134. B.P. Xiao, C. E. Reece, M.J. Kelley, Superconducting surface impedance under radiofrequency field, *Physica C* **490**, 26 (2013).
135. C. E. Reece, A. D. Palczewski, B. P. Xiao, An analysis of the temperature and field dependence of the RF surface resistance of nitrogen-doped niobium SRF cavities with respect to existing theoretical models, in *Proc. of IPAC2015*, Richmond VA USA (2015). www.jacow.org.
136. G. Ciovati, P. Dhakal, A. Gurevich, Decrease of the surface resistance in superconducting niobium resonator cavities by the microwave field, *Appl. Phys. Lett.* **104**, 092601 (2014).
137. D. Gonnella, M. Ge, F. Furuta, and M. Liepe, Nitrogen treated cavity testing at Cornell, in *Proc. of LINAC2014*, Geneva, Switzerland (2014). www.jacow.org.
138. J. T. Maniscalco, D. Gonnella, and M. Liepe, The importance of the electron mean free path for superconducting radio-frequency cavities, *J. Appl. Phys.* **121**, 043910 (2017).
139. D. Gonnella, F. Furuta, M. Ge, J. Kaufman, P.N. Koufalas, M. Liepe, and J.T. Maniscalco, Dependence of surface resistance of N-doping level, in *Proc. of IPAC2016*, Busan, Korea (2016). www.jacow.org.
140. S. Sridhar and J. E. Mercereau, Non-equilibrium dynamics of quasiparticles in superconductors, *Phys. Rev. B* **34**, 203 (1986).
141. A. Gurevich and T. Kubo, Surface impedance and optimum surface resistance of a superconductor with imperfect surface, *Phys. Rev. B* **96**, 184515 (2017).
142. A. Gurevich, Theory of rf superconductivity for resonant cavities, *Supercond. Sci. Technol.* **30**, 034004 (2017).
143. J. R. Delayen, H. Park, S. U. De Silva, G. Ciovati, and Z. Li, Determination of the magnetic field dependence of the surface resistance of superconductors from cavity tests, *Phys. Rev. Accel. Beams* **21** 122001 (2018).
144. T. Kubo, Physics and challenges of superconducting cavities for particle accelerators and theoretical implication towards higher performance, *J. Cryo. Soc. Jpn.* **54**, 275 (2019)
145. T. Kubo, and A. Gurevich, Field-dependent nonlinear surface resistance and its optimization by surface nanostructuring in superconductors, *Phys. Rev. B* **100** 064522 (2019)
146. W. P. M. R. Pathirana, and A. Gurevich, Nonlinear dynamics and dissipation of a curvilinear vortex driven by a strong time-dependent Meissner current, *Phys. Rev. B* **101** 064504 (2020).
147. T. Kubo, Weak-field dissipative conductivity of a dirty superconductor with Dynes subgap states under a dc bias current up to the depairing current density, *Phys. Rev. Research* **2** 013302 (2020)
148. M. Martinello, M. Checchin, A. Romanenko, A. Grassellino, S. Aderhold, S. K. Chandrasekeran, O. Melnychuk, S. Posen, and D. A. Sergatskov, Field enhanced superconductivity in high frequency niobium cavities, *Phys. Rev. Lett.* **121**, 224801 (2018).
149. P. Dhakal, Status of infusion studies at Jlab, in *presentation at TTC2020*, Feb 4-7, 2020, Geneva, Switzerland.
150. R. Eichhorn, D. Gonnella, G. Hoffstaetter, M. Liepe, W. Weingarten, On superconducting niobium accelerating cavities fired under N₂-gas exposure, *preprint arXiv:1407.3220* (2014).
151. M. Ge, F. Furuta, M. Liepe, G. H. Hoffstaetter, Field dependent surface resistance of a superconducting RF cavity caused by surface impurity, *arXiv preprint arXiv:1507.08704* (2015).
152. A. Blais, R-S. Huang, A. Wallraff, S. M. Girvin, and R. J. Schoelkopf, Cavity quantum electrodynamics for superconducting electrical circuits: An architecture for quantum computation, *Phys. Rev. A* **69**, 062320 (2004).
153. R. J. Schoelkopf and S. M. Girvin, Wiring up quantum systems, *Nature* **451**, 664 (2008).
154. H. Paik *et al.*, Observation of high coherence in Josephson junction qubits measured in a three-dimensional circuit QED architecture, *Phys. Rev. Lett.* **107**, 240501 (2011).
155. R. Janish, V. Narayan, S. Rajendran, and P. Riggins, Axion production and detection with superconducting rf cavities, *Phys. Rev. D* **100**, 015036 (2019).
156. A. Romanenko, R. Pilipenko, S. Zorzetti, D. Frolov, M. Awida, S. Belomestnykh, S. Posen, and A. Grassellino, Three-Dimensional Superconducting Resonators at T<20 mK with Photon Lifetimes up to $\tau=2$ s, *Phys. Rev. Applied* **13**, 034032 (2020).

-
157. S. Posen, and M. Liepe, Advances in development of Nb₃Sn superconducting radio frequency cavities, *Phys. Rev. ST Accel. Beams* **17**, 112001 (2014).
 158. S. Posen, M. Liepe, and D. L. Hall, Proof-of-principle demonstration of Nb₃Sn superconducting radiofrequency cavities for high Q_0 applications, *Appl. Phys. Lett.* **106**, 082601 (2015).
 159. G. Ereemeev, W. Clemens, K. Macha, C.E. Reece, A.M. Valente-Feliciano, S. Williams, U. Pudasaini, M. Kelley, Nb₃Sn multicell cavity coating system at JLAB, in *arXiv preprint*, *arXiv:2001.03823* (2020).
 160. G. Ciovati *et al.*, Design of a cw, low-energy, high-power superconducting linac for environmental applications, *Phys. Rev. Accel. Beams* **21**, 091601 (2018).
 161. A. Gurevich, Enhancement of rf breakdown field of superconductors by multilayer coating, *Appl. Phys. Lett.* **88**, 012511 (2006).
 162. A. Gurevich, Maximum screening fields of superconducting multilayer structures, *AIP Advances* **5**, 017112 (2015).